

The hybrid path planning algorithm based on improved A* and artificial potential field for unmanned surface vehicle formations

Hongqiang Sang^a, Yusong You^a, Xiujun Sun^{b,*}, Ying Zhou^c, Fen Liu^a

^a School of Mechanical Engineering and Tianjin Key Laboratory of Advanced Mechatronic Equipment Technology, Tiangong University, Tianjin, 300387, China

^b Physical Oceanography Laboratory, Ocean University of China, Qingdao, 266100, China

^c Institute for Advanced Ocean Study, Ocean University of China, Qingdao, 266100, China

ARTICLE INFO

Keywords:

USV formation
A* global path planning
Multiple sub-target APF local path planning
USV dynamics

ABSTRACT

To effectively improve system autonomy, increase fault-tolerant resilience, solve low payload capacity and short endurance time of unmanned surface vehicles (USVs), there's a trend to deploy multiple USVs as a formation fleet. The formation path planning algorithms are essential to generate optimal trajectories and provide practical collision avoidance maneuvers to efficiently navigate the USV fleet. To ensure the optimality, rationality and path continuity of the formation trajectories, this paper presents a novel deterministic algorithm named multiple sub-target artificial potential field (MTAPF) based on an improved APF. The MTAPF belongs to the local path planning algorithm, which refers to the global optimal path generated by an improved heuristic A* algorithm, and the optimal path is divided by this algorithm into multiple sub-target points to form sub-target point sequence. The MTAPF can greatly reduce the probability that USVs will fall into the local minimum and help USVs to get out of the local minimum by switching target points. As an underactuated system, the USV is restricted by various motion constraints, and the MTAPF is presented to make the generated path compliant with USV's dynamics and orientation restrictions. The proposed algorithm is validated on simulations and proven to work effectively in different environments.

1. Introduction

In recent years, with the benefits of autonomy technology as well as the driving demand of autonomous vehicles collaborate with each other, there has been an increasing development of unmanned surface vehicles (USVs). The applications of USVs include military utilizations such as sea patrol (Bertaska et al., 2015) and coastal guarding (Han et al., 2015), as well as civilian or scientific deployments such as environmental monitoring (Sharma et al., 2014) and bathymetric survey (Rimon and Koditschek, 1992a). However, current USV platforms are greatly limited for low payload capacity and short endurance times under complex tasks. Multiple vehicles as a formation fleet that allows cooperative operations to be deployed will be the trend of current and future USV operations. In some specific tasks, maintaining proper formation can improve work efficiency, speed up the completion of target tasks, reduce system consumption, and enhance the robustness of USV formation fleet system.

For USV cooperative operation, it is especially important to march

according to an optimal path with the highest efficiency and robustness. A formation path planning strategy to be studied needs to meet the following indicators (Qu et al., 2008):

- Rationality: Any returned path is reasonable, or any path is executable for controlling USV formation fleet operations.
- Completeness: If there is a collision-free path from a starting point to an end point, an algorithm can be found. If there is no path in the environment, a planning failure will be reported.
- Optimality: The planned path is optimal for a certain measurement such as time, distance, or energy consumption.
- Real time: The formation path planning algorithm can be performed in real time, which can respond quickly and meet time requirements.

The cooperative formation controls are focused on how to maintain or track the desired positions and orientations relative to a defined reference point (Shojaei, 2015). The control strategies including the leader-follower control (Chen et al., 2010), the virtual structure

* Corresponding author.

E-mail addresses: sanghongqiang@tiangong.edu.cn (H. Sang), onepiece_yo@163.com (Y. You), sxj@ouc.edu.cn (X. Sun), yingzhou@ouc.edu.cn (Y. Zhou), liufen@tiangong.edu.cn (F. Liu).

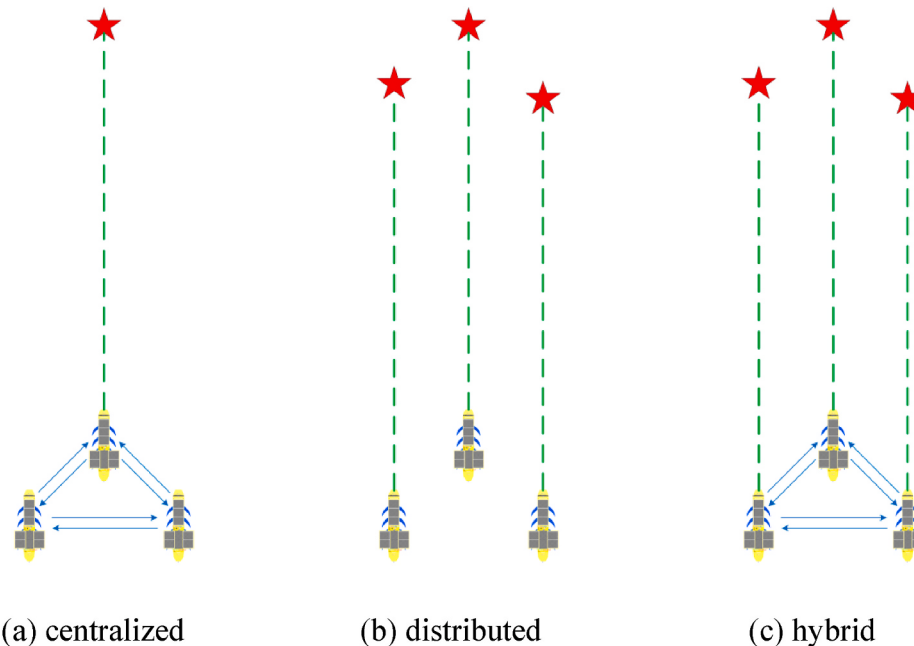


Fig. 1. Centralized, distributed and hybrid control strategies.

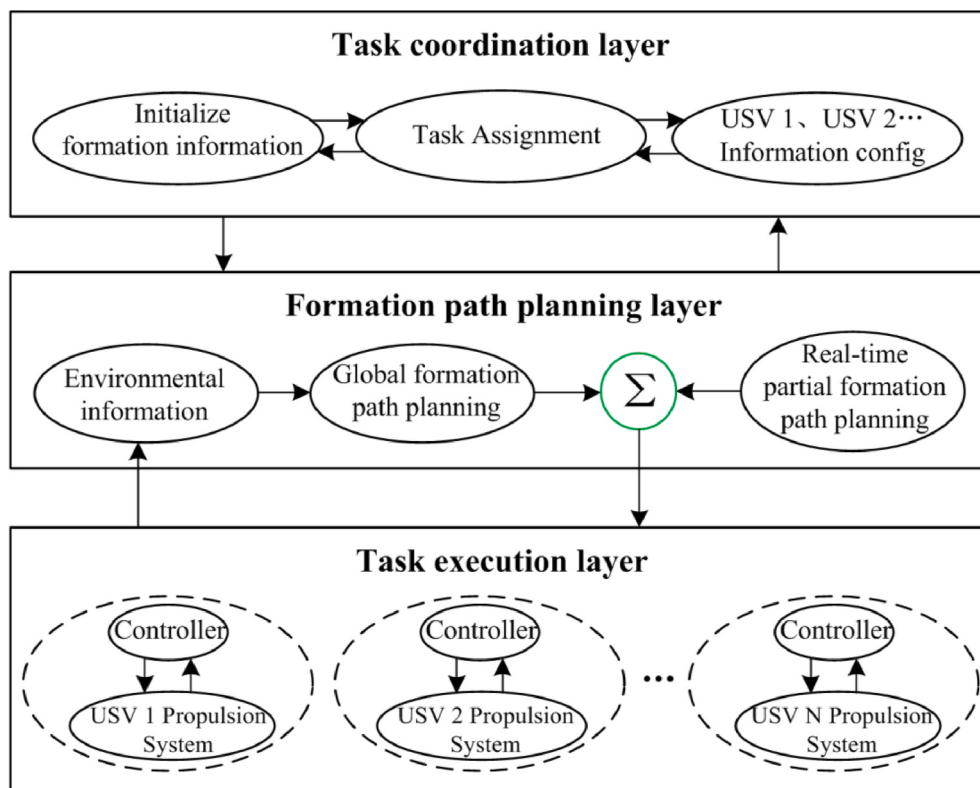


Fig. 2. Hierarchy structure of multiple USVs system.

approach ([Mehrjerdi et al., 2011](#)) and the behavior-based formation control ([Oberleithner et al., 2012](#)) are widely used. In some high-level autonomous behaviors such as collision avoidance can also be fulfilled by adding additional controllers ([Mahacek et al., 2012](#)).

Fig. 1 describes the control strategies, which is the core of maintaining the performance of the formation. The red star indicates the target point, the dashed line indicates the ideal path, and the blue arrow indicates data interaction. The collaborative control system composed of

multiple USVs can be divided into three types: centralized, distributed and hybrid (Jialiang, 2012). Centralized control refers to the integration of mission planning information and formation information into one of USVs. The USV is used as the leader, other USVs act as the followers. The leader coordinates the action of each follower to keep a formation to reach a target point. The shortcoming of this control system is that once the leader has an unexpected situation in the formation, the entire formation will be disbanded and the task cannot be completed. Therefore,

the control strategy has less robustness and fault-tolerant resilience. Distributed control is that each USV has the ability of independently receiving commands and analysis. Each USV can decide the action according to own wishes and communicate with the monitoring center on the shore to report information such as the location and velocity at the time. Because they cannot communicate with each other, the coordination efficiency of multiple USVs is low and local conflicts are easy to occur, which will cause that the overall situation is poor.

Hybrid control system takes into account the advantages of centralized and distributed control strategies such as agility, flexibility and reliability. The continuity and robustness are better, which can meet the needs of multiple USVs collaborative work.

Generally speaking, a hierarchical structure of USV formation system consists of three layers, i.e. task coordination layer, formation path planning layer and task execution layer, which is shown in Fig. 2. The task coordination layer transmits planning information such as the USV formation information and the each USV position information to the formation path planning layer. The formation path planning layer sends the planned position, expected heading and velocity of the planned sub-target points to the task execution layer, and motion control can be accomplished by the controller. Feedback mechanisms are set up among all levels to correct deviations. The task coordination layer is responsible for all task assignments, formation information configuration, formation design, and initialization of each USV control system. A global path planning and a real-time local path planning are performed according to the environmental information obtained by sensors in the formation path planning layer. According to the feedback information of the path planning, the execution layer of each USV controls the USV to perform propeller propulsion and turning.

The formation path planning is a complicated task and can be viewed as a multi-objective optimization problem. The planned trajectory should be optimized in terms of several aspects such as total distance, navigation time and energy consumption. Although formation path planning methods for unmanned aerial vehicle (UAV), unmanned ground vehicle (UGV) and mobile robots are studied (Qiu and Duan, 2014; Zuo et al., 2016), there is few works focused on developing a robust formation path planning algorithm for USVs (Liu and Bucknall, 2015). Obstacles like islands and buoys in the ocean increase the complexity and difficulty of formation path planning, thus the planned path must be smooth, continuous and feasible, and dynamic constraints should also be considered when the USV marches according to the planned path.

The nature of USV formation path planning is an optimization process of multiple objectives, which is more complicated than single vehicle path planning (Liu and Bucknall, 2015). The formation path planning needs to consider internal collision avoidance, formation shape keeping, cooperation behavior, formation shape change, and total path distance. To achieve formation path planning, a number of different approaches have been proposed, which can be categorized as two disciplines (Liu and Bucknall, 2015):

- Heuristic approach
- Deterministic approach

The heuristic method can be used to speed up the process of finding a satisfactory solution (Liu and Bucknall, 2015; Cheekuang et al., 2009). In general, the heuristic method requires a large amount of computation and long computation time, and is rarely used in applications where real-time requirements are high. Since the heuristic method does not follow a rigorous process, the results generally vary. The process is mostly uncertain, so it has a high degree of randomness.

The USV is researched in this paper. The propeller is used for forward driving and the rudder is used for heading control. Different specifications of the USV have different endurance capabilities. The listed path planning algorithms in this paper are not only limited to the USV, but also other equipment. A number of heuristic algorithms such as genetic

Table 1
Relevant methods for USVs formation.

Methods	Main features
Traditional APF	Generating path without considering optimality; Easy to fall into local minima problem
APF + Virtual structure (Pan et al., 2017)	Effectively maintain formation shape; Without considering path optimality; Easy to fall into local minima problem
APF + Kane's method (Yang et al., 2011)	A multi-body system; Stable formation shape; Jumping out of the local minimum; Introducing AUV dynamics and only for AUV
DAPF (Niizuma et al., 2015)	Real-time planning and stable formation shape; Non-optimal path
ACO + APF (Liu et al., 2015)	Solving the problems of slow convergence speed in the ACO and the local optimum in the APF; Obtaining a global path; Does not give an optimal principle
PSO (Bai et al., 2009)	Optimal time for forming formation shape; Unable to maintain a stable formation shape
Genetic algorithm (Qu et al., 2013)	Global path planning; The path is optimal in some respects; Without real-time path planning
FMM (Garrido et al., 2011; Gomez et al., 2013)	Avoiding local minima problem; Higher path continuity; Poor keeping formation shape; Non-optimal path
Traditional A* (Hao and Agrawal, 2005)	Long search time; A large of iterations and calculation
Theta* (Kim et al., 2014)	Introducing the turning rate of the USV; Larger calculations and calculation time
IA*+MTAPF(ours)	Taking into account the USV kinematic constraints; The shortest distance principle; Real-time planning; Jumping out of the local minimum

algorithm, particle swarm optimization and ant colony asexual reproduction optimization have been researched (Wang et al., 2019). A novel hybrid diversity particle swarm optimization (PSO) and time optimal control approach was proposed for multiple unmanned aerial vehicles (multi-UAVs) formation reconfiguration in dynamic and complicated environments (Bai et al., 2009). This method belongs to a heuristic algorithm, which can find a feasible path in a complex environment. The path is more optional, and can meet the optimal solution of a certain principle. However, the forming process of the formation shape is only considered, the maintenance of the formation is not premeditated in these algorithms, and this algorithm needs a large amount of calculation and time. An improved genetic algorithm with co-evolutionary strategy was put forward for the global path planning of multiple mobile robots (Qu et al., 2013). The global path planning algorithm can be used to ensure that the path is optimal in some respects, but it does not meet real-time requirement. In addition, there are some hybrid algorithms such as combining an ant colony algorithm with an APF algorithm. The local force factor of the APF was converted into spreading pheromones in the ant searching process (Liu et al., 2015) and the ant colony algorithm focused on subspace search with high fitness. This algorithm can solve the problems of slow convergence speed in ant colony algorithm and the local optimum in artificial potential field method. However, the ultimate goal of this algorithm is to obtain a global path, which does not give an optimal principle. A fast marching method (FMM) was employed to generate trajectories for mobile robot formation (Garrido et al., 2011; Gomez et al., 2013). An improved FMM was used to deal with the collision avoidance problem of moving vessels in a practical maritime environment (Liu and Bucknall, 2015). The FMM algorithm provides a good smoothness and continuity path, however it still does not fully address the dynamic constraints, especially without considering the vehicles' heading angles (Qu et al., 2008), and the planning path is not optimal. A novel angular rate constrained algorithm was proposed based on Theta* (Kim et al., 2014), which was a grid-based method and was similar to A*. The feasible points in the space were redefined by introducing the turning rate of the USV, however long calculation time was needed.

The deterministic algorithms have the characteristics of search

completeness and consistency. The APF is becoming a main method due to its easy implementation and good collision avoidance (Liu and Bucknall, 2016). The APF method was initially used to plan the global optimal trajectory for an individual robot in an obstacle environment (Perdereau et al., 2002; Rimon and Koditschek, 1992b). A motion planning and obstacle avoidance of multiple hybrid-driven underwater glider (HUG) formation using the APF method and Kane's method was presented (Yang et al., 2011). The HUG uses the net buoyancy and attitude angle adjustment to obtain propulsion. It consumes little energy when adjusting the net buoyancy and attitude angle, which shows the characteristics of high efficiency and long endurance (up to thousands of kilometers). The HUG formation with an APF was regarded as a multi-body system, in which the HUG was constrained by the virtual forces derived from the APF. The problems of collision and the global minimum point were solved by a dynamic artificial potential field (DAPF) based on the local information (Niizuma et al., 2015). The APF is a local path planning algorithm and has the advantages of real-time planning and stable formation shape, but the planned path is not optimal. The main drawback of the APF is suffering from the local minima problem. Once the formation falls into the local minimum area and the USV receives the same amount of gravity and repulsive force, the formation will not be able to march and the mission will fail. The formation algorithms and main features are shown in Table 1.

The deterministic algorithm considers the path planning problem from the conventional perspectives and not to consider simultaneously time cost, distance cost and obstacle avoidance (Qu et al., 2008). The heuristic path planning algorithm is not able to rigorously maintain the formation shape. The uncertainty and randomness of the heuristic search makes the path hard follow a predefined shape and the heuristic path planning suffers from incompleteness and inaccuracy of search results (Liu and Bucknall, 2015).

A multiple sub-target artificial potential field (MTAPF) is put forward in this paper, which combines an improved A* heuristic global path planning algorithm and an improved APF deterministic algorithm. The improved A* heuristic global path planning algorithm is used to generate the optimal path, and the optimal path is divided into multiple sub-target point sequence. The improved APF deterministic algorithm is used to keep the formation shape. In the local path planning, the referenced optimal path makes the formation have higher motion efficiency. During obstacle avoidance, the marching path is more continuous, smooth and complete. The MTAPF can greatly reduce the probability of the formation falling into the local minimum and help USVs to get out of the local minimum by switching the target point. When two obstacles approach, the formation can pass through the narrow passage by using the MTAPF. The orientation of USV at the start of the march and the feasible constrained route within the vehicle's turning capability have been considered in the MTAPF path planning algorithm.

The rest of the paper is organized as follows. Section 2 describes the global path planning strategy based on the improved A* algorithm. Section 3 gives the local path planning algorithm based on the improved APF. Section 4 puts forward the USV formation path planning algorithm based on the MTAPF. Section 5 verifies the proposed algorithms and strategies. Section 6 concludes this paper and discusses the future work.

2. The global path search algorithm based on the improved A*

The proposed hybrid path planning algorithm is mainly composed of two parts: global path planning algorithm and local formation path planning algorithm. In this section, the improved A* is used as the global path planning algorithm to generate an optimal path, which guides the USV formation to reach the target point quickly and safely. Furthermore, the comparison between traditional A* and the proposed improved A* is carried out.

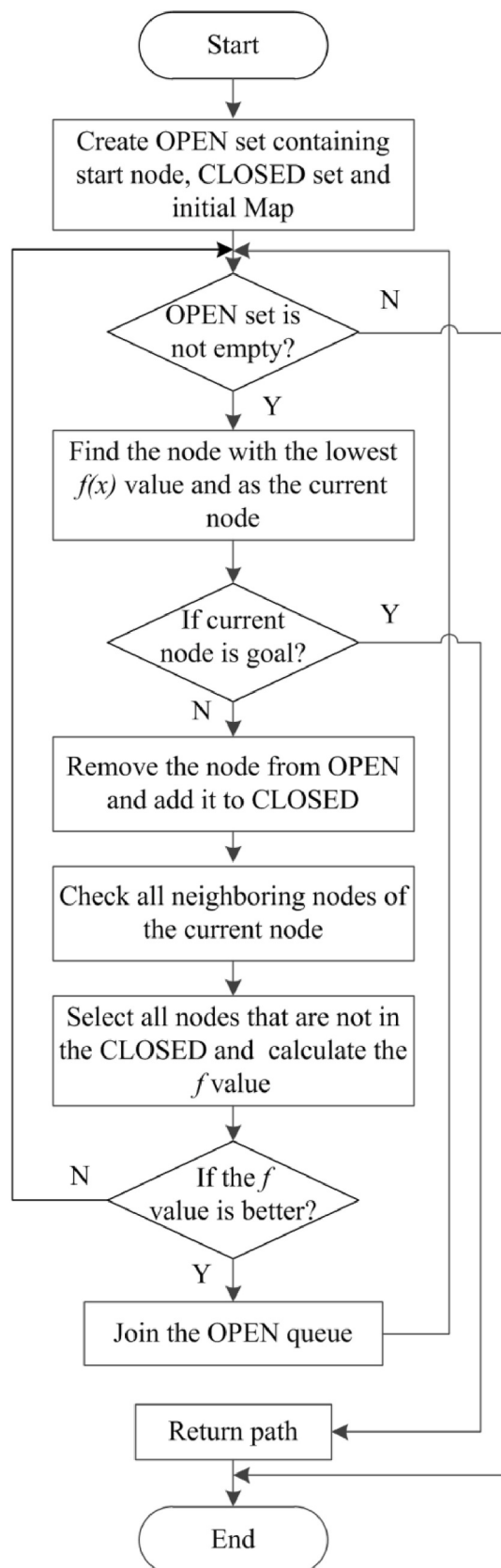


Fig. 3. The flow chart of the A* algorithm.

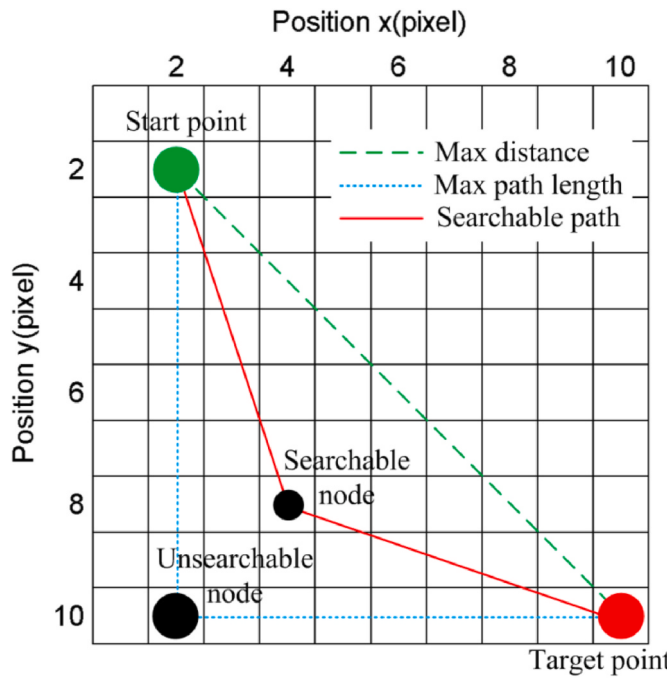


Fig. 4. Maximum search distance and maximum path length constraints.

2.1. Traditional A* for global path planning

A^* is an informed incremental heuristic search algorithm, or a popular variant of best-first search. The algorithm was firstly published in 1968 (Hart et al., 1972). A formation path planning framework with the A^* algorithm was firstly proposed for unmanned ground vehicles in a dynamic environment.

As a classical grid-based methodology, the A^* has been widely applied in different shapes and forms. A heuristic method is used to search towards the goal position in the A^* algorithm. The A^* algorithm can find the shortest path by using an edge cost and a heuristic based on the Euclidean distance (Hao and Agrawal, 2005). Although the A^* algorithm can ensure to generate the shortest path, the smoothness and continuity of the path need be improved to strictly follow the shortest path. Meanwhile the A^* algorithm can still not fully solve the dynamic constraint problem, especially without considering the vehicles' heading angle change. Under the condition of the vehicle's dynamics, the local path planning of the formation need refer to the path generated by the global path planning algorithm to improve the smoothness and continuity of the path.

In each iteration of its main loop, the A^* need determine which node to extend, which bases on the cost of the path and the estimated cost of extending the path all the way to the goal point. Specifically, the A^* selects the path that minimizes:

$$f(n) = g(n) + h(n) \quad (1)$$

where n is the next node on the path, $g(n)$ is the cost of the path from the starting node to n , and $h(n)$ is a heuristic function that estimates the cost of the cheapest path from n to the goal node.

If the heuristic function is admissible, this means that the A^* can return a least-cost path from the starting node to the goal node and it will never overestimate the actual cost to arrive at the goal node.

A typical implementation of the A^* is to repeatedly select the minimum estimated cost node to be expanded by using a priority queue. This algorithm can divide all the found nodes into two sets:

- OPEN: This priority queue is known as an OPEN set, and is the set of currently found nodes that are yet not evaluated.

- CLOSED: The node set has already been evaluated.

Fig. 3 gives the flow chart of the A^* algorithm. At each step of the algorithm execution, the node with the lowest value $f(x)$ is removed from the queue, and these neighbors that are not in CLOSED are added to the queue, and the values of f and g are updated. The algorithm will stop until the queue is empty or a goal node is found in the queue. h is zero at the goal node, so f value is the cost of the shortest path. After running this algorithm, the end node will point to its previous node until the previous node of some nodes becomes the starting node.

2.2. The improved A^* algorithm

Traditional A^* algorithm cannot guarantee the safety of the vehicle, and has a large amount of calculation. It does not consider the shortcomings of the turning cost and the redundant path points. Therefore, the following improvements are carried out.

- (a) Reduce search points near obstacles and keep a safe distance to avoid collision. Traditional A^* algorithm converts the map into a binary map and then obtains a grid map, but it does not simplify the grid near an obstacle. In the search process, not only the search area is increased, but also the obtained path is closer to the obstacle. The safety of the USV cannot be guaranteed when avoiding obstacles.
- (b) The maximum search distance and maximum path length constraint are shown in Fig. 4, which limits maximum search distance to reduce search range and shorten search time. During the search process, the straight line distance from the starting point to the target point is defined as the maximum distance L_{md} , and L_{mp} is the maximum path length through the node. The added search constraints are

$$\begin{cases} h(n) \leq k \cdot L_{md} \\ f(n) \leq \lambda \cdot L_{mp} \end{cases} \quad (2)$$

where k and λ are the scale factors.

- (c) The turning cost $h(\delta)$ is added into the heuristic function to avoid frequent turns of the USV and improve the smoothness of the path. To reduce the path turning points and avoid the roundabout and frequent turning of the USV, the turning cost is added into the heuristic function.

$$f(n) = g(n) + h(n) + h(\delta) \quad (3)$$

- (d) A trajectory optimization algorithm is proposed to optimize the generated trajectory, eliminate redundant points and shorten the path length. The obtained path is equally divided by the optimization algorithm. It is determined as a redundant path point by judging if there are obstacles around each path point.

The running processes and the planned paths based on the A^* algorithm and the improved A^* algorithm are shown in Fig. 5. It can be seen from Fig. 5(a) and (c) that the number of nodes based on the improved A^* algorithm is less and the distance from the obstacles is larger. The red path is optimized by the trajectory optimization algorithm and the blue path is not optimal path in Fig. 5(d). It can be seen from Fig. 5(b) and (d) that the path length based on the improved A^* algorithm is shorter. The operation information of the A^* algorithm is given in Table 2, compared with the improvement before, the path length has been reduced by 3.2%, the search time has been reduced by 30.5%, and the number of search nodes has been reduced by 9.3%. For the planned path, the A^* algorithm can ensure the shortest path and is optimal from the perspective of distance, however the A^* algorithm does not fully consider the dynamic constraints of USVs especially heading angle

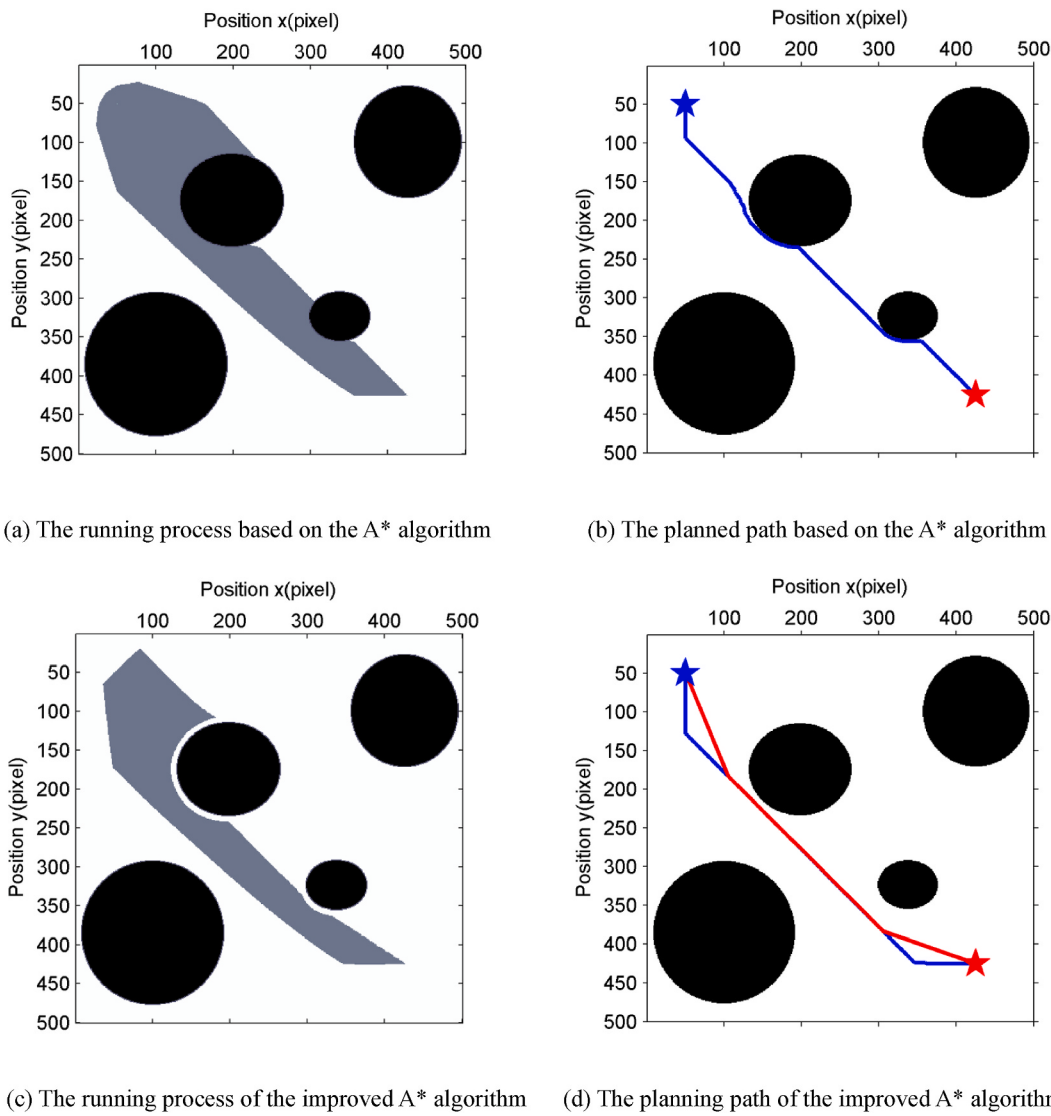


Fig. 5. The running processes and the planned paths based on the A* algorithm and the improved A* algorithm.

Table 2

The operation information of the A* algorithm.

	Binary Map (pixel)	starting Position (pixel)	Goal Position (pixel)	Path Length (pixel)	Time (s)	Number of nodes
A*	500 × 500	(50,50)	(425,425)	571	118	1413
improved A*	500 × 500	(50,50)	(425,425)	553	82	1282

changes. The formation local planning path refers to the global path rather than strictly following the global path, which improves the smoothness and continuity of the planned path.

3. The local path planning algorithm based on the improved APF

The optimal path obtained by the global path planning algorithm is divided into multiple sub-target point sequences and the formation shape is formed and maintained well considering the obstacles. The local path planning algorithm is presented, the traditional APF and the proposed improved APF are discussed in detail in this section.

3.1. Traditional and the improved APF for path planning

As a deterministic path planning algorithm, the APF algorithm has the advantages of more maturation, more efficiency, and simple mathematical calculation, and has been widely used. As an effective local path planning algorithm, the APF constructs a potential field in the working environment of mobile robot, and the mobile robot is affected by gravitational field of the target and a repulsion of surrounding obstacles (Kuppan Chetty et al., 2012). However, when using traditional APF for path planning, there are mainly three problems:

- (a) Because traditional artificial potential field method uses a virtual force to control the movement of a USV, when two obstacles are close to each other, the USV may not be able to pass through the narrow passage. In addition, the obstacle and the target point are on the same line, the force control of the USV can only move repeatedly on the straight line, but cannot reach the target point.
- (b) In the case of only one target point, when a USV has not arrived, the gravity of the target point to the USV is likely be equal to the repulsive force of the obstacle to the vehicle. When the resultant force is zero, the USV will fall into local minimum and stop marching.

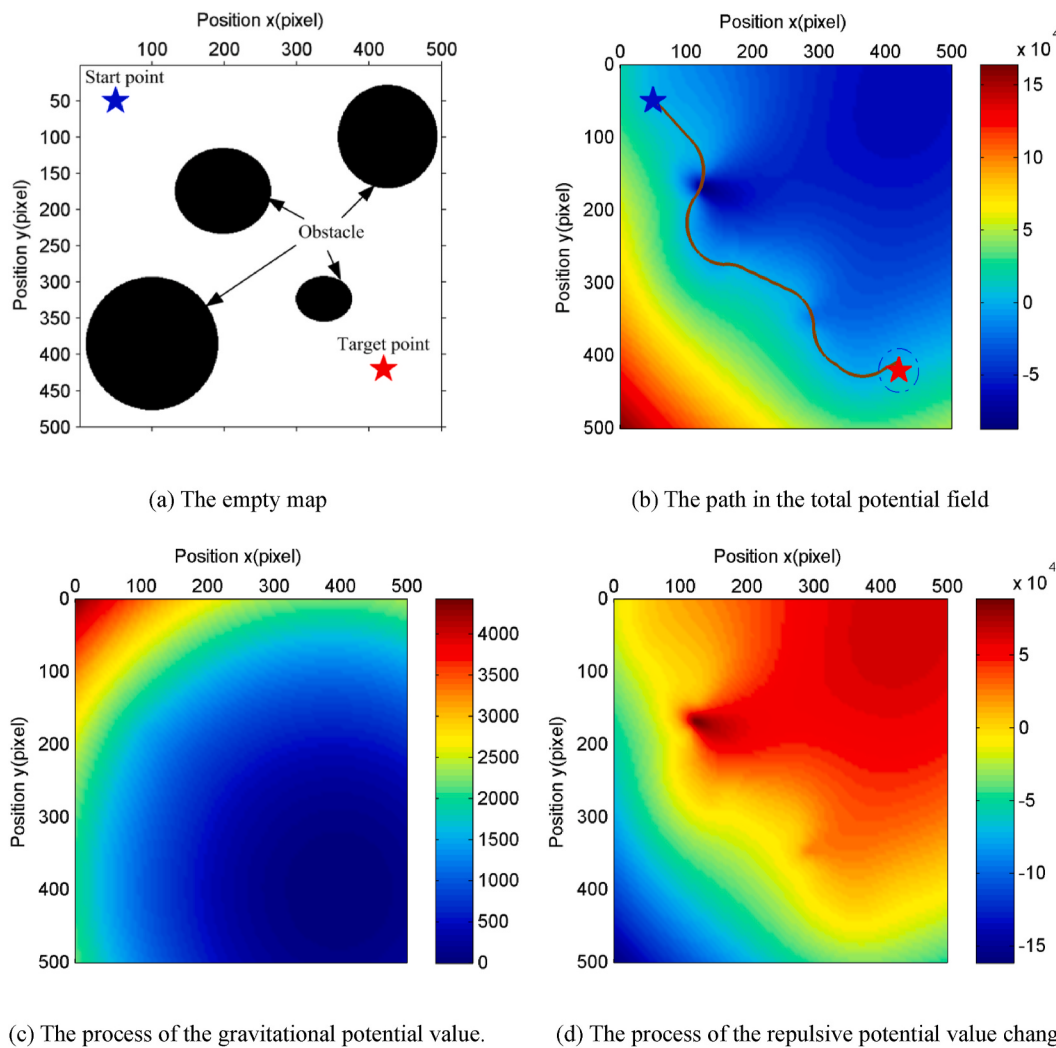
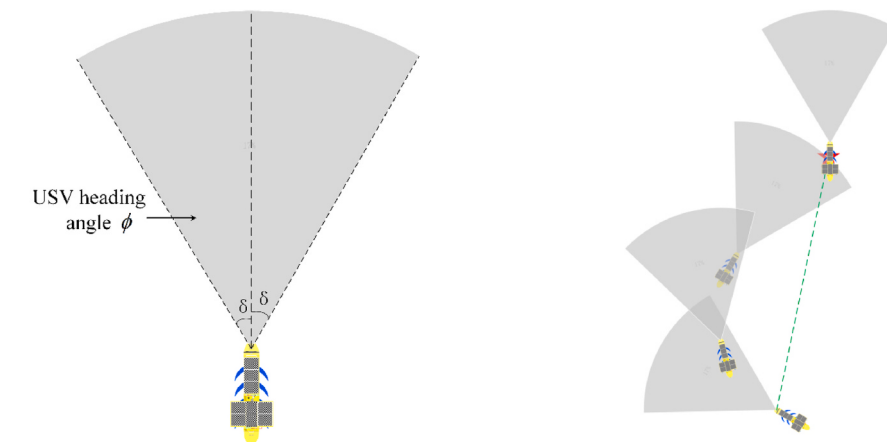


Fig. 6. The APF algorithm running description graph.

(c) In the case of only one target point, although the trajectory of the USV conforms to the dynamic limitation, its trajectory does not satisfy the optimal conditions such as the shortest path and the least time. During the travel process, it is greatly affected by environmental factors.

In view of the shortcomings of traditional APF algorithm, the following improvements are performed:

(a) The gravitational field of the target to the USV and the repulsive field of the obstacle to the USV are transformed into potential



(a) The USV's turning angle and heading angle

(b) The movement under the USV dynamic constraints

Fig. 7. The dynamic description of the USV.

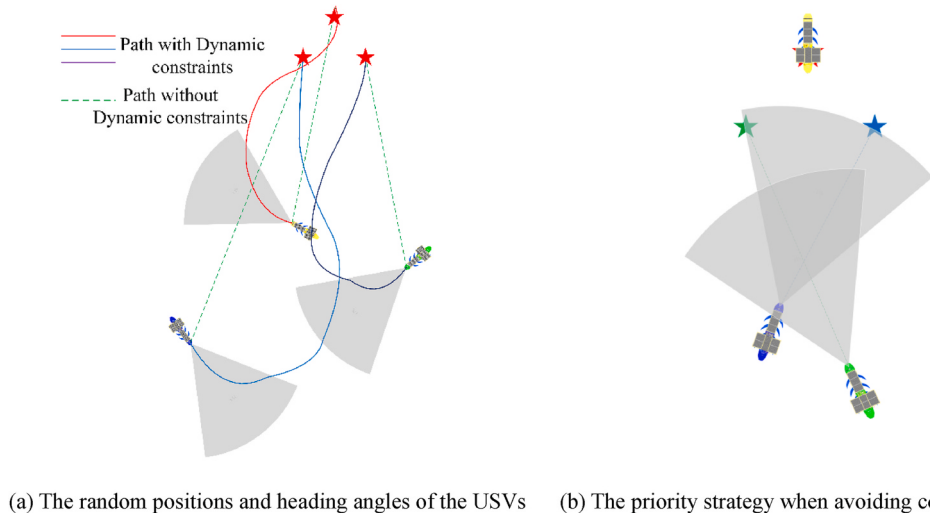


Fig. 8. The march paths of the USVs and the priority strategy under dynamic constraints.

- field strength. The traditional vector force control is replaced by the calculation of potential field strength.
- (b) Combined with the improved A* algorithm, a novel MTAPF algorithm is put forward. In the path planning of the USV, the sequence of sub-target points is formed by dividing multi-target points, which greatly reduces the probability that a USV falls into a local minimum. Even if the USV falls into local minimum, and the velocity of the USV is close to zero. At this time, finding the next target point in the sequence of sub-target points as the current target point can help the USV get out of the local minimum.
- (c) The division of multi-target points refers to the global optimal path obtained by the improved A* algorithm, so that the USV

formation trajectory can be optimized under the condition of satisfying the dynamic constraints of the USV.

3.2. The improved APF model

Through the above improved measurements, an improved APF model is established. The gravitational potential field model of goal point to moving USV is

$$U_{attr} = \lambda_{attr} \cdot [\rho(X, G)]^k \cdot [\sin \theta(X, G), \cos \theta(X, G)] \quad (4)$$

where $\rho(X, G)$ is the distance from current point $X(x, y)$ to goal point $G(x, y)$. λ_{attr} is a scaling factor for gravitational potential field and has a minimum amount $\lambda_{minattr}$, which is greater than zero. $k = 2.5$ is an index of calculating field. $\theta(X, G)$ is an angle between current point $X(x, y)$ and goal point $G(x, y)$.

The repulsive potential field model of goal point to moving USV is

$$U_{rep} = \lambda_{rep} \cdot \left[\frac{1}{\rho(X, O)} \right]^k \cdot [\sin \theta(X, O), \cos \theta(X, O)] \quad (5)$$

where $\rho(X, O)$ is the distance from current point $X(x, y)$ to obstacle point $O(x, y)$. λ_{rep} is a scaling factor for repulsive potential field and has a minimum amount λ_{minrep} , which is greater than zero. $k = 2$ is an index of calculating potential field. $\theta(X, O)$ is an angle between current point $X(x, y)$ and obstacle point $O(x, y)$. The obstacle is respectively located in the front, left, right, left front, right front of the USV, the angle between the USV and the obstacle should also be changed.

$$U_{total} = U_{attr} - U_{rep} \quad (6)$$

where U_{attr} is the gravitational potential filed, U_{rep} is the repulsive potential field, and U_{total} is the total potential field.

Under the action of the total potential field, the USV begins to march with the kinetic model. Fig. 6(a) shows an empty 500×500 pixel map. Fig. 6(b) gives the change process of the total potential field, the potential value is given by Equation (6) and the solid brown line is the path generated by the APF. Fig. 6(c) and (d) give the change of gravitational potential field and the repulsive potential field, respectively. The gravitational potential value and the repulsive potential value are respectively calculated by using Equations (4) and (5).

During the formation process, due to the different total potential fields are received by a single USV, it may happen that a certain USV in the formation cannot reach the goal point in time, and multiple USVs in the formation may collide. The cooperation of multiple USVs in the formation will be discussed in detail in the next section.

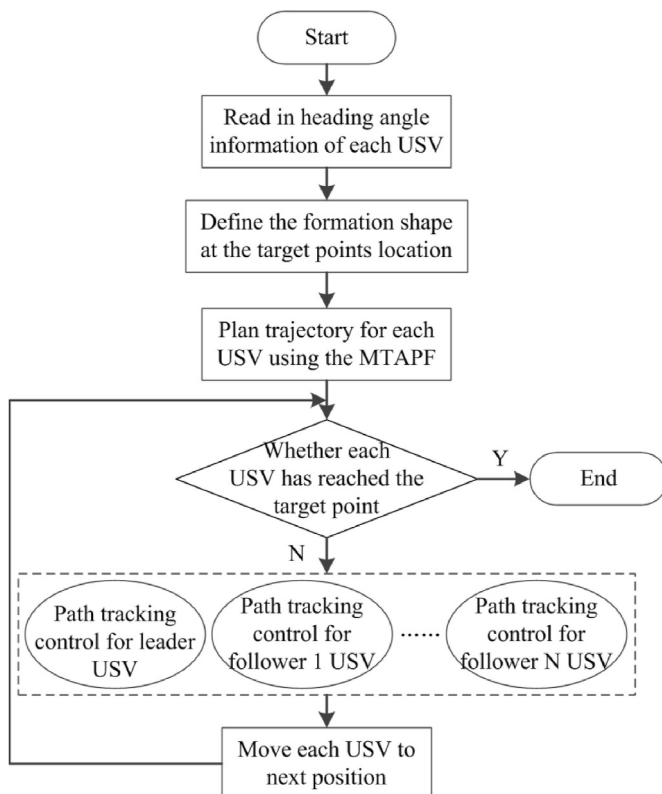


Fig. 9. The flow chart of the USV formation algorithm.

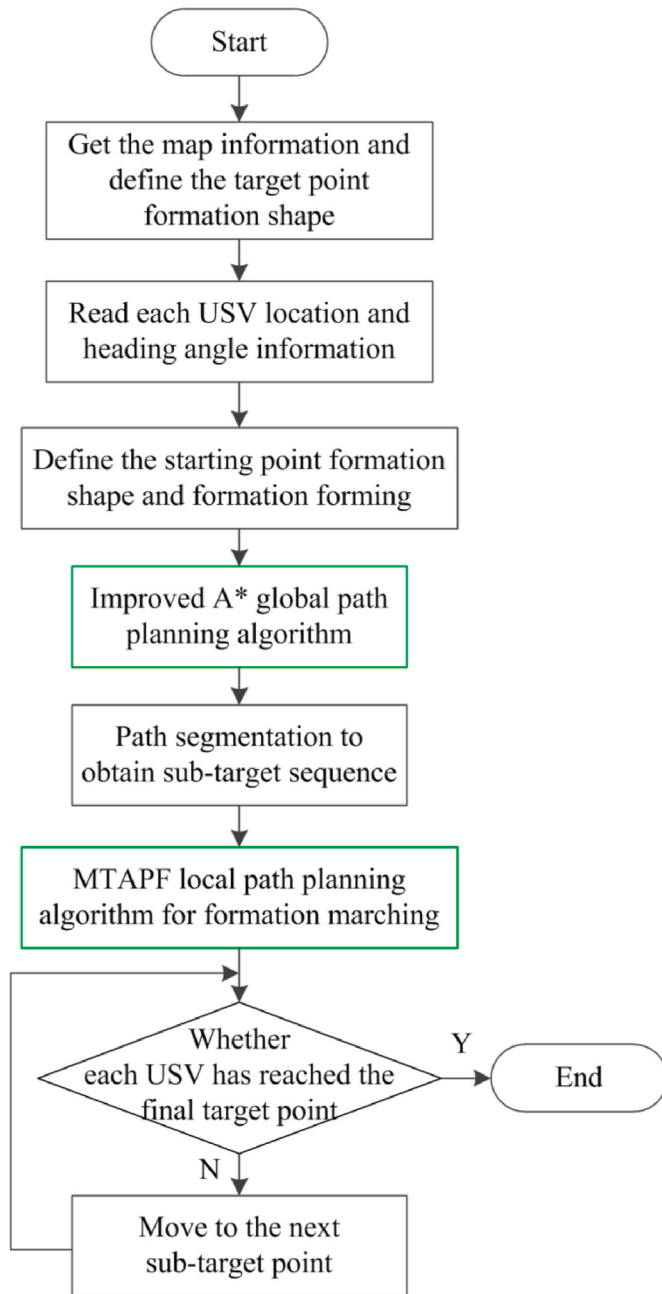


Fig. 10. The flow chart of the formation path planning algorithm.

4. The USV formation path planning based on the MTAPF and the improved A* algorithm

In this section, a dynamic model of the USV is used as the motion simulation plant for the proposed control algorithm. The global path planning control (the improved A* algorithm) and the local multiple sub-target artificial potential field (MTAPF) considering the dynamic constraints are combined as the hybrid path planning algorithm, and the control process is described in detail.

4.1. The motion equation of the USV

When an USV moves on a horizontal plane, it is usually described as consisting of three free moving parts: surge, sway and yaw (Wang and Xu, 2020). The 3 degree of freedoms (DOFs) nonlinear dynamic model of

the USV can be expressed as:

$$\dot{\eta} = \mathbf{J}(\eta)\mathbf{v} \quad (7)$$

$$\mathbf{M}\dot{\mathbf{v}} + \mathbf{C}(\mathbf{v})\mathbf{v} + \mathbf{D}(\mathbf{v})\mathbf{v} = \boldsymbol{\tau} \quad (8)$$

where $\eta = [x \ y \ \psi]^T$ is a position vector, $\mathbf{v} = [u \ v \ r]^T$ is a velocity vector, $\boldsymbol{\tau}$ is a control input, $\mathbf{J}(\eta)$ is a transformation matrix between an earth-fixed frame and a body-fixed frame. \mathbf{M} is an inertia matrix, \mathbf{C} is a Coriolis and centripetal matrix, \mathbf{D} is a linear damping matrix. The parameters are defined as follows:

$$\mathbf{J}(\eta) = \begin{pmatrix} \cos \psi & -\sin \psi & 0 \\ \sin \psi & \cos \psi & 0 \\ 0 & 0 & 1 \end{pmatrix} \quad \mathbf{M} = \begin{pmatrix} m - X_u & 0 & 0 \\ 0 & m - Y_v & mx_g - Y_r \\ 0 & mx_g - Y_r & I_z - N_r \end{pmatrix}$$

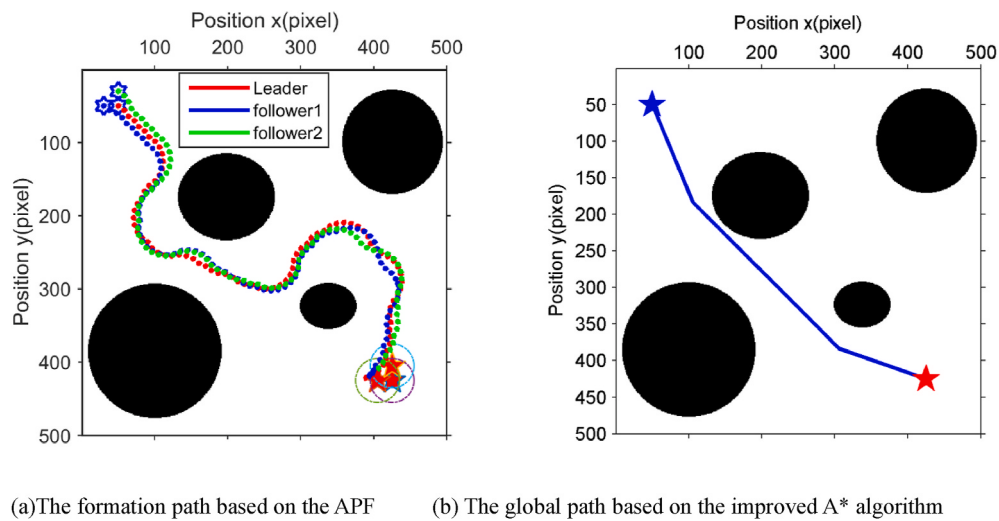


Fig. 11. The APF algorithm and the improved A* algorithm path graph.

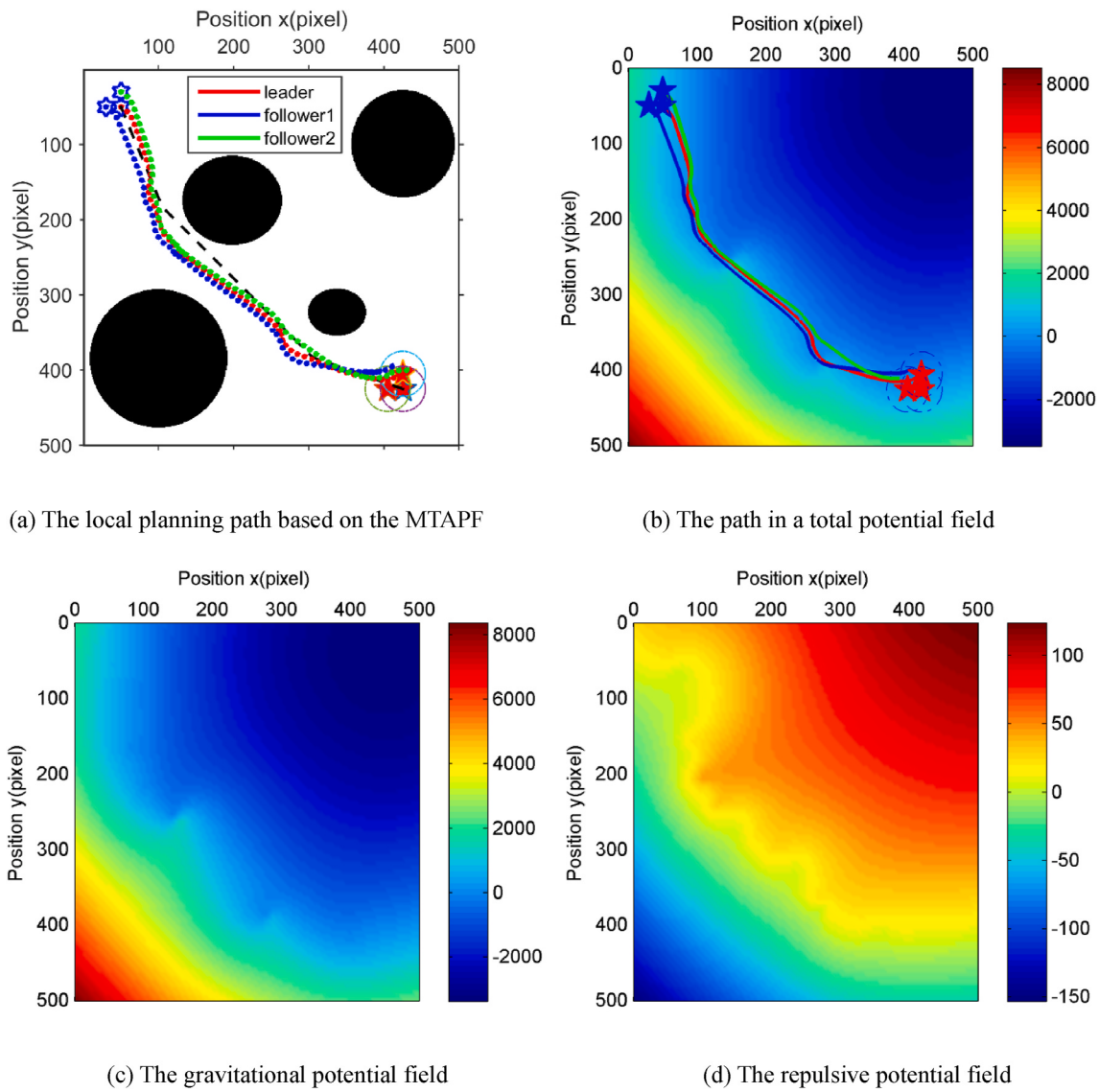
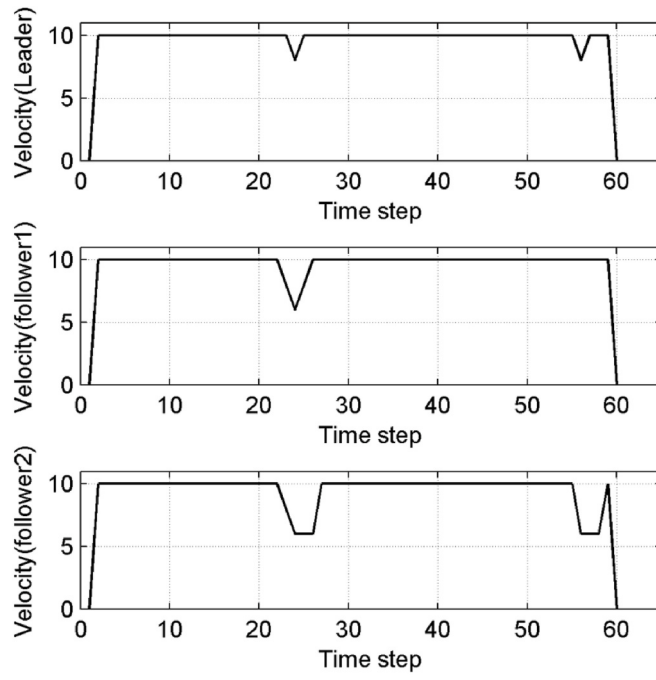
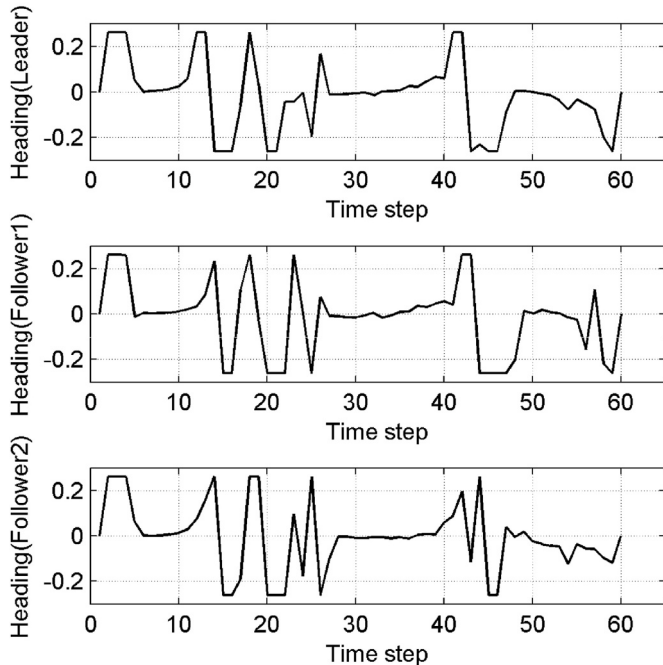


Fig. 12. The MTAPF algorithm path and potential field graph.



(a) The velocity curves of the leader and two followers



(b) The heading curves of the leader and two followers

Fig. 13. The velocity and the heading curves of the USVs.

$$\mathbf{C} = \begin{pmatrix} 0 & 0 & -(m - Y_v)v - (mx_g - Y_r)r \\ 0 & 0 & (m - X_u)u \\ (m - Y_v)v + (mx_g - Y_r)r - (m - X_u)u & 0 \end{pmatrix}$$

$$\mathbf{D} = \begin{pmatrix} -X_u & 0 & 0 \\ 0 & -Y_v & -Y_r \\ 0 & -N_v & -N_r \end{pmatrix}$$

Equation (8) is transformed into the earth-fixed frame, which can be expressed as:

Table 3

The formation path lengths of the USVs under different algorithms.

Algorithm	Leader USV path length (pixel)	Follower 1 USV path length (pixel)	Follower 2 USV path length (pixel)
Improved APF	779	792	791
Improved A*	553	N/A	N/A
MTAPF	728	728	723

Table 4

The configuration parameters of the USV formation.

USV	Initial position (pixel)	Goal (pixel)	Initial heading (rad)	Max velocity (pixel/time step)	Max turning (rad)
Leader USV	(50,50)	(425,425)	$\pi/8$	10	$15 \times \pi/180$
Follower 1 USV	(50,30)	(425,405)	$\pi/8$	10	$15 \times \pi/180$
Follower 2 USV	(30,50)	(405,425)	$\pi/8$	10	$15 \times \pi/180$

$$\mathbf{M}_\eta(\eta)\ddot{\eta} + \mathbf{C}_\eta(v, \eta)\dot{\eta} + \mathbf{D}_\eta(v, \eta)\dot{\eta} = \tau_\eta \quad (9)$$

where

$$\mathbf{M}_\eta(\eta) = \mathbf{J}^{-T}(\eta)\mathbf{M}\mathbf{J}^{-1}(\eta), \quad \mathbf{C}_\eta(v, \eta) = \mathbf{J}^{-T}(\eta)[\mathbf{C}(v) - \mathbf{M}\mathbf{J}^{-1}(\eta)\mathbf{j}(\eta)]\mathbf{J}^{-1}(\eta), \quad \tau_\eta = \mathbf{J}^{-T}(\eta)\tau$$

$$\mathbf{D}_\eta(v, \eta) = \mathbf{J}^{-T}(\eta)\mathbf{D}(v)\mathbf{J}^{-1}(\eta)$$

Equation (9) is rewritten as the following format:

$$\ddot{\eta} = \mathbf{M}_\eta^{-1}(\eta)[\mathbf{J}^{-T}(\eta)\tau - \mathbf{C}_\eta\dot{\eta} - \mathbf{D}_\eta\dot{\eta}] \quad (10)$$

Assuming that $u = \mathbf{J}(\eta)\mathbf{M}^{-1}\tau$ is a virtual control variable. Then, Equation (10) can be expressed as:

$$\ddot{\eta} = -\mathbf{M}_\eta^{-1}(\eta)[\mathbf{C}\eta\dot{\eta} + \mathbf{D}\eta\dot{\eta}] + u \quad (11)$$

As the USV is underactuated and the vehicle can only be controlled in the surge and yaw motions. The surge velocity u is taken into account and specified as:

$$u \leq u_{max} \quad (12)$$

where u_{max} is a maximum surge velocity.

In addition, the USV has a limited turning capability, thus the vehicle's yaw rate is:

$$|r| \leq r_{max} \quad (13)$$

where r_{max} is the maximum yaw rate of the USV.

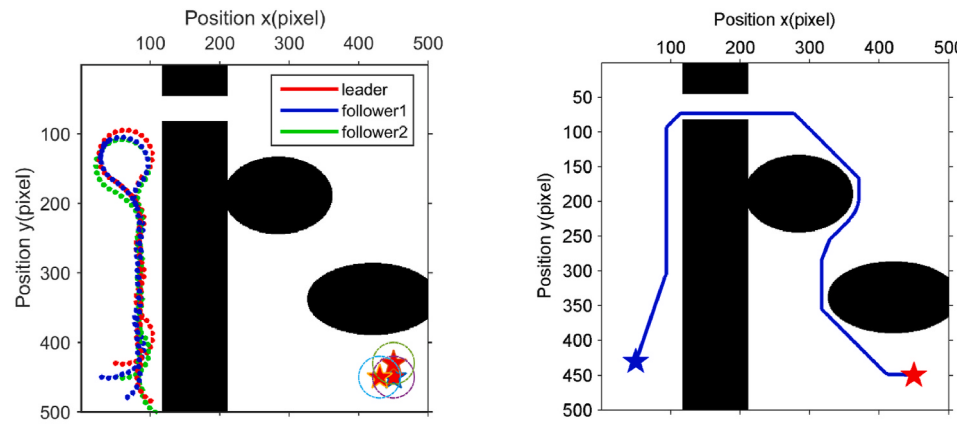
4.2. The dynamic constraints and priority strategy of the USV

The USV is underactuated during most of operation time, which makes it have low maneuverability and motion flexibility (Liu and Bucknall, 2016). Special consideration should be given to a heading angle problem. The USV's turning angle is shown in Fig. 7(a), and the turning angle δ is described as:

$$\delta = r_{max}\Delta T \quad (14)$$

where ΔT is the control interval time.

The path considering the USV dynamic constraints is shown in Fig. 7(b), where the dashed line indicates the path without dynamic



(a) The formation marching in a narrow environment (b) The global planning path by using the improved A*

Fig. 14. The traditional APF algorithm and the improved A* algorithm in narrow complex environment.

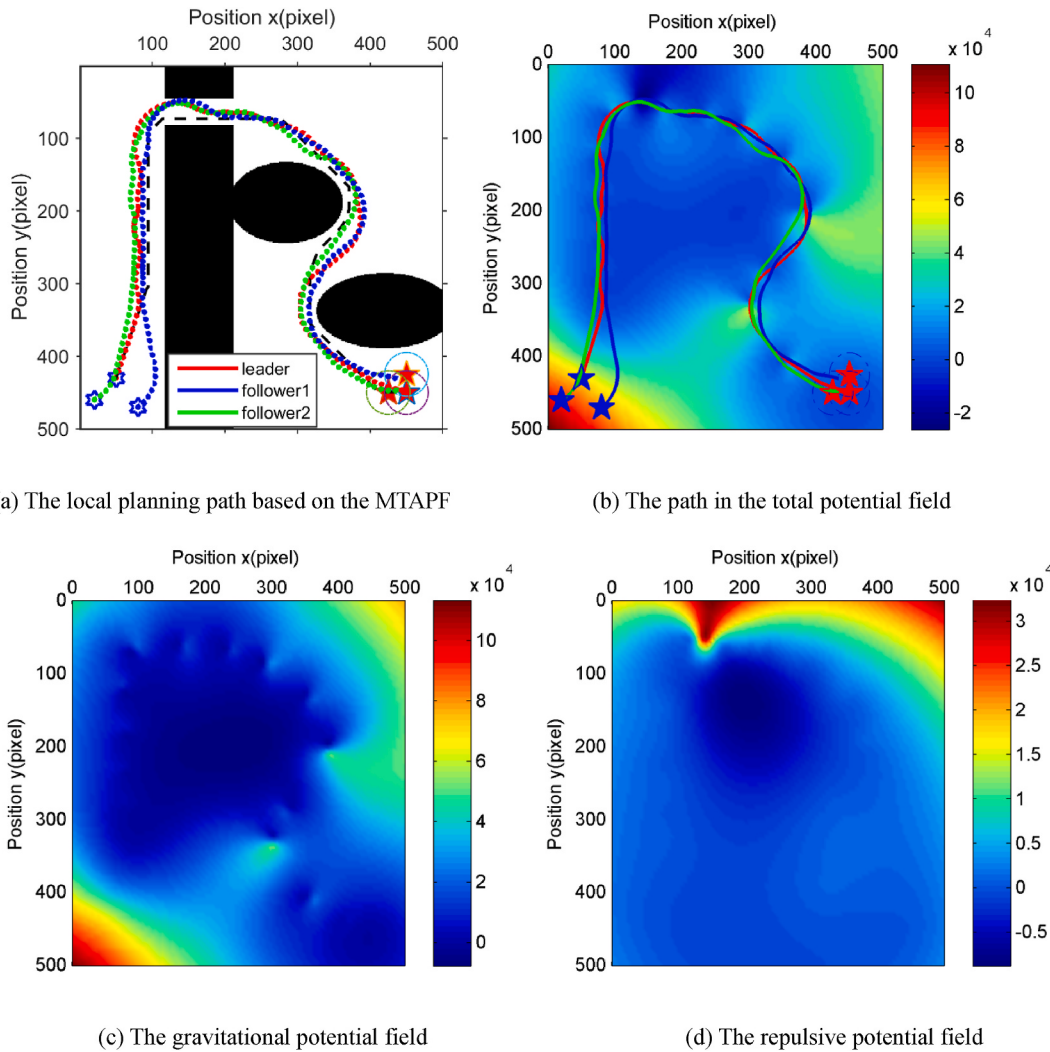


Fig. 15. The MTAPF algorithm path and potential field in narrow complex environment.

constraints. Because of the limitation of turning ability, the USV is limited under the dynamic conditions, which will result in an undesirable path. Therefore, the dynamic characteristics of the USV must be considered when planning the USV path.

The smoothness and continuity of the path should be considered. In addition, it is also considered whether the dynamic constraints of the USV are met, especially the initial heading angle. The USV's position and the heading angle are random during the USV deployment. When

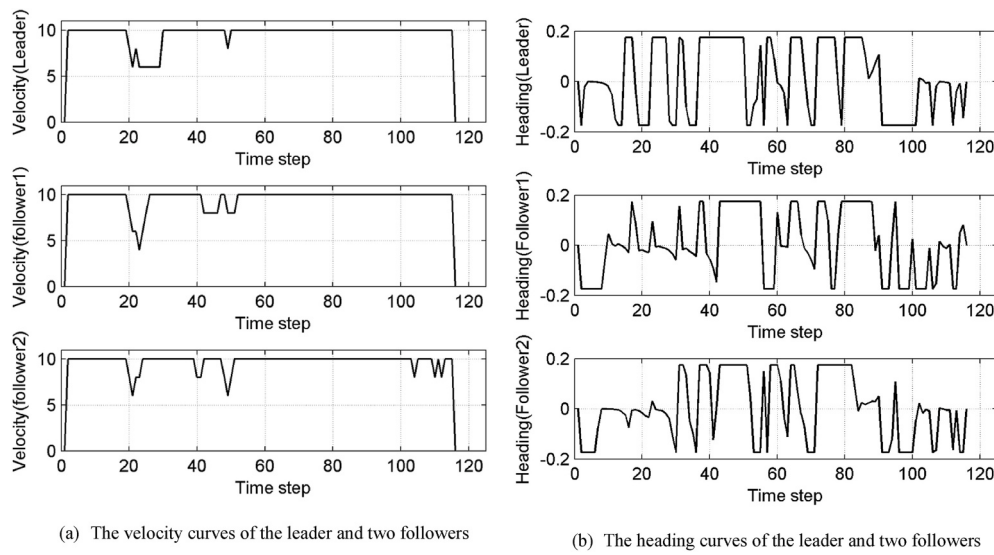


Fig. 16. The velocity curves and the heading curves of the USVs.

the formation shape is formed, each USV moves toward a target point, which is as shown in Fig. 8(a). The solid line is the path of the USV with dynamic limitation, and the dash line is the path of the USV without dynamic limitation. Considering the dynamic constraints, the simulation results are more realistic. Therefore, to verify the importance of dynamic constraints, dynamic constraints and non-dynamic constraints need be distinguished.

When the USV starts to deploy, its position and heading are not in accordance with the expectation. Therefore, the positions and the heading angles of the various USVs are random before the formations shape is formed. When the distance between two USVs is too close, collisions may occur. The priority strategy is adopted to avoid collisions during the formation forming process. As seen in Fig. 8(b), the yellow USV is the leader, and the green USV farthest from the leader is designated as sub-follower. When the distance between the sub-follower and the follower (the blue USV) is small, the velocity of sub-follower is slow. In contrast, the sub-follower starts to accelerate.

4.3. The MTAPF algorithm for the USV formation forming and path planning

The MTAPF is multiple sub-target APF algorithm based on the improved APF algorithm. When the formation plans paths, the MTAPF algorithm refers to the path generated by the improved A* algorithm, and then divides multi-target points to form a sub-target point sequence. In the stage of the formation forming, an algorithm based on the MTAPF is proposed, and the flow chart of the algorithm is shown in Fig. 9. When the algorithm starts to work, the initial heading angle of each USV is first read. Leader-follower approach is used to design the formation shape, and one USV from the formation is selected to guide the motion of the

Table 5

The formation path lengths of USVs in a narrow environment under different algorithms.

Algorithm	Leader USV path length (pixel)	Follower 1 USV path length (pixel)	Follower 2 USV path length (pixel)
Traditional APF	N/A	N/A	N/A
Improved A*	1066	N/A	N/A
MTAPF	1099	1076	1024

formation. The second step is to get the leader's target point position and calculate the follower's target points according to the formation parameters. The MTAPF is then applied to each USV to generate the appropriate trajectory based on the assigned target point. Path tracking control is executed by each USV until the target point is reached.

The trajectory tracking tasks will be performed after the trajectories are generated. It is assumed that each USV has a trajectory tracking controller such that its individual path can be perfectly tracked without errors. The assumption is reasonable and has been applied to formation path planning (Álvarez et al., 2015).

Fig. 10 gives the flow chart of the formation path planning algorithm, which is developed based on the MTAPF and uses a binary map.

Step one, define the USVs' starting points and goal points and read the information of each USV because USVs have random initial heading angles and positions. Step two, execute the formation shape forming algorithm. Step three, once the formation shape is finished and each USV has arrived the starting point, the improved A* algorithm starts a global path planning algorithm to obtain an optimal path and sub-target point sequence. Step four, the MTAPF algorithm starts a local formation path planning algorithm based on the dynamic constraints of the USV. [Algorithm 1](#) is the MTAPF algorithm. In [Algorithm 1](#), M is the initialized map, P_{start} is the starting point, and P_{goal} is the target point. For different USVs in the formation, the starting point and the target point are different, which facilitates the formation of the formation. $P_{location}$ is the current position point of each USV, $P_{heading}$ is the current heading of each USV, and the path set is the set of various path points. After the formation is formed, the improved A* global path planning algorithm is used to obtain a global path, and the sub-target points of the target path

Table 6

The random configuration parameters of the USV formation.

USV	Initial position (pixel)	Goal (pixel)	Initial heading (rad)	Max velocity (pixel/time step)	Max turning (rad)
Leader USV	(430,50)	(450,450)	$-\pi/3$	10	$10 \times \pi/180$
Follower 1 USV	(470,80)	(425,450)	$-\pi/6$	10	$10 \times \pi/180$
Follower 2 USV	(460,20)	(450,425)	$-\pi/8$	10	$10 \times \pi/180$

can be obtained by dividing the global path. Before reaching the final target point, taking the sub-target point as the current formation target point, the MTAPF algorithm is used to advance to reach the final target point.

Require: Map (M), Starting point (P_{start}), Goal point (P_{goal}).

- 1: $M :=$ an empty map;
- 2: $P_{start} := \{P_{leader}, P_{follower1}, \dots, P_{followern}\};$
- 3: $P_{goal} := \{P_{leader}, P_{follower1}, \dots, P_{followern}\};$
- 4: $P_{location} := \{P_{leader}, P_{follower1}, \dots, P_{followern}\};$
- 5: $P_{heading} := \{P_{leader}, P_{follower1}, \dots, P_{followern}\};$
- 6: Path := [];
- 5: **while** ~has formation shape been formed
- 6: formation shape forming algorithm ($P_{location}, P_{heading}$);
- 7: **end**
- 8: Path \leftarrow the improved A* global path planning algorithm (M);
- 9: subGoal[n] \leftarrow Path;
- 10: **while** ~has reached the P_{goal}
- 11: **for** (int i = 0; i < subGoal.length; i++)
- 12: GoalPoint \leftarrow subGoal[i];
- 13: **while** ~has reached the GoalPoint
- 14: MTAPF local formation path planning algorithm (GoalPoint);
- 15: **end**
- 16: **end**
- 17: **end**

Algorithm 1. Multiple sub-target artificial potential field algorithm

5. Algorithm validations

This section discusses and analyses the simulation results under two different environments. The main indicators of the comparison results are: arriving the target point, the length of the path, and time to complete the task, real-time, the smoothness and continuity of the path. When the formation is planned, the planned path and trajectory tracking must meet the dynamic characteristics of the USV. The obstacles are described in black color in all simulation results.

5.1. Formation path planning in a complex environment

The formation path planning in a complex environment is shown in Fig. 11. When the APF algorithm is used for the local path planning, the formation cannot refer to the path in Fig. 11(a). The lengths of the path are long and the smoothness of the formation path is poor. The global

path planning based on the improved A* algorithm is shown in Fig. 11 (b), and the blue path is the generated optimal path. It can be clearly seen that the optimal path is relatively short and smooth.

The local path planning based on the MTAPF is shown in Fig. 12 (a),

which refers to the global planning path by using the improved A* algorithm. Where the red line is the trajectory of the leader, the blue line is that of the follower 1, and the green line is that of the follower 2. Fig. 12 (b)–(d) give the total potential field, the gravitational potential field and the repulsive potential field, respectively. It can be seen that the length of the formation path is short and the continuity and smoothness of the formation path are high, when the improved A* algorithm is used for the global path planning and the MTAPF algorithm is used for the local path planning.

Fig. 13 gives the velocity and the heading curves of the leader, the followers 1 and 2 in the formation. The comparison results are given in Table 3. The path length with the improved A* algorithm is 30.2% less than that with the APF algorithm. Moreover, the path with MTAPF algorithm is reduced by a maximum of 8.1% compared with the APF algorithm. N/A means that no path planning is performed in Table 3. A global optimal reference path can be obtained only once, thus there is no need to perform plan planning again. In the case of a long voyage, the effect of the algorithm will be more obvious. Table 4 gives the information of each USV in this simulation.

5.2. Formation path planning in a narrow passage

The formation marching in a narrow intricate environment is shown in Fig. 14. It can be seen from Fig. 14(a) that the formation based on traditional APF cannot pass through the narrow passageway.

When the repulsive potential is greater than the gravitational potential, the formation is trapped in the local space. When the repulsive potential is equal to the gravitational potential in some field, the formation will fall into a local minimum and stop marching. Thus, the above-mentioned problems must be considered when the formation performs tasks. In a centralized control system, when the leader in the formation falls into a local minimum or fails, the entire formation will be paralyzed. In this paper, a hybrid control system is adopted, which increases the robustness and reliability of the system. Fig. 14(b) gives the global planning path by using the improved A* algorithm.

The MTAPF algorithm path and potential field in narrow complex environment are show in Fig. 5.

Fig. 15(a) gives the local planning path based on the MTAPF in a narrow complex environment which refers to the global planning path by using the improved A* algorithm. Fig. 15(b) gives the formation paths in the total potential field. The formation passes through the narrow passageway smoothly with continuous trajectory. When forming the formation shape, the position and the heading of each USV are randomly distributed. After the formation, the formation begins to march. When constructing a local planning path, the priority strategy is adopted to prevent collision. Fig. 15(c)-(d) gives the gravitational potential field and the repulsive potential field, respectively. It can be seen from Fig. 15(d) that the closer the USV is to the obstacle, the greater the repulsion potential.

Fig. 16 gives the velocity and the heading curves of the leader, the followers 1 and 2 in the formation. The formation path lengths of USVs in a narrow environment under different algorithms are given in Table 5. The APF algorithm cannot be used to reach the target point through a narrow passage. The N/A indicates that there is no path length and the path planning is not completed. The formation can be carried out with the A* and MTAPF algorithms. Because the voyage is longer, the path length is correspondingly longer. Table 6 gives the random configuration parameters of the USV formation. The difference from Table 4 is that the initial heading and position of each USV are random.

6. Conclusions and future works

A new MTAPF algorithm based on the improved APF was put forward, and the formation path selection of the USV, robustness and reliability in marching were analyzed in this paper. The improved A* algorithm was adopted to obtain the optimal path and the MTAPF algorithm was used to carry out the local path planning, which ensured the forming of the formation shape, the maintenance of formation shape and the robustness and reliability of formation. Under the premise of satisfying the dynamic characteristics of the USVs, the continuity and the smoothness of the path were assured. When constructing a local planning path, a priority strategy was used to prevent from colliding with each other. A hybrid control system was adopted and the leader-follower control strategy controls the formation collaboration of multiple USVs. Simulation results verified the effectiveness of the proposed algorithm.

In terms of the future work, the proposed algorithms will be implemented on the practical USV platforms, and the global and the local path planning controllers will be designed. After the prototype is completed, sea trials will be performed. Besides the practical vehicle is verified, the dynamic environment need be deeply researched, which includes various moving ships associated with different encounter situations. In addition, the dynamic environment can also refer to the varying environment that may be affected by ocean conditions such as currents and tides. In the dynamic environment, the path planning and collision avoidance strategies of the USV formation will be the main work in

future.

CRediT authorship contribution statement

Hongqiang Sang: Conceptualization, Data curation, Formal analysis, Funding acquisition. **Yusong You:** Investigation, Methodology, Formal analysis, Project administration, Validation, Visualization, Writing - review & editing. **Xiujun Sun:** Formal analysis, Resources, Supervision, Funding acquisition. **Ying Zhou:** Formal analysis, Software, Roles/Writing - original draft. **Fen Liu:** Formal analysis, Writing - review & editing.

Declaration of competing interest

The authors declare that they have no known competing financial interests or personal relationships that could have appeared to influence the work reported in this paper.

Acknowledgments

This research is supported by Tianjin Natural Science Foundation (No.18JCZDJC40100), Major Scientific and Technological Innovation Projects of Shandong Province (No.2019JZZY020701), the National Key Research and Development Plan of China (No.2017YFC0305902), Wenhui Program of Qingdao National Laboratory for Marine Science and Technology (No.2017WHZZB0101), and the Program for Innovative Research Team in University of Tianjin (No. TD13-5037).

References

- Álvarez, D., Gómez, J.V., Garrido, S., et al., 2015. 3D robot formations path planning with fast marching square. *J. Intell. Rob. Syst.* 80 (3-4), 1–17.
- Bai, C., Duan, H., Member, S., et al., 2009. Dynamic multi-UAVs formation reconfiguration based on hybrid diversity-PSO and time optimal control. In: *Intelligent Vehicles Symposium*. IEEE, pp. 775–779.
- Bertaska, I.R., Shah, B., Von, E.K., et al., 2015. Experimental evaluation of automatically-generated behaviors for USV operations. *Ocean Eng.* 106, 496–514.
- Cheekuang, T., Richard, B., Alistair, G., 2009. Review of collision avoidance and path planning methods for ships in close range encounters. *J. Navig.* 62 (3), 22.
- Chen, J., Sun, D., Yang, J., et al., 2010. Leader-follower formation control of multiple non-holonomic mobile robots incorporating a receding-horizon scheme. *Int. J. Robot Res.* 29 (6), 727–747.
- Garrido, S., Moreno, L., Lima, P.U., 2011. Robot formation motion planning using Fast Marching. *Robot. Autonom. Syst.* 59 (9), 675–683.
- Gomez, J.V., Lumbier, A., Garrido, S., et al., 2013. Planning robot formations with fast marching square including uncertainty conditions. *Robot. Autonom. Syst.* 61 (2), 137–152.
- Han, J., Park, J., Kim, T., et al., 2015. Precision navigation and mapping under bridges with an unmanned surface vehicle. *Aut. Robots* 38 (4), 349–362.
- Hao, Y., Agrawal, S.K., 2005. Planning and control of UGV formations in a dynamic environment: a practical framework with experiments. *Robot. Autonom. Syst.* 51 (2), 101–110.
- Hart, P.E., Nilsson, N.J., Raphael, B., 1972. A formal basis for the heuristic determination of minimum cost paths. *IEEE Trans. Syst. Sci. Cybern.* 4 (37), 28–29.
- Jialiang, L.I., 2012. Development and application of unmanned surface vehicle. *Fire Control Command Control* 37 (6), 203–207.
- Kim, H., Kim, D., Shin, J.U., et al., 2014. Angular rate-constrained path planning algorithm for unmanned surface vehicles. *Ocean Eng.* 84 (4), 37–44.
- Kuppan Chetty, R.M., Singaperumal, M., Nagarajan, T., 2012. Behavior based multi robot formations with active obstacle avoidance based on switching control strategy. *Adv. Mater. Res.* 433–440, 6.
- Liu, Y., Bucknall, R., 2015. Path planning algorithm for unmanned surface vehicle formations in a practical maritime environment. *Ocean Eng.* 97, 126–144.
- Liu, Y., Bucknall, R., 2016. The angle guidance path planning algorithms for unmanned surface vehicle formations by using the fast marching method. *Appl. Ocean Res.* 59, 327–344.
- Liu, J., Yang, J., Liu, H., et al., 2015. Robot global path planning based on ant colony optimization with artificial potential field. *Trans. Chin. Soc. Agric. Mach.* 46 (9), 18–27.
- Mahacek, P., Kitts, C.A., Mas, I., 2012. Dynamic guarding of marine assets through cluster control of automated surface vessel fleets. *IEEE ASME Trans. Mechatron.* 17 (1), 65–75.
- Mehrjerdi, H., Ghommag, J., Saad, M., 2011. Nonlinear coordination control for a group of mobile robots using a virtual structure. *Mechatronics* 21 (7), 1147–1155.
- Niizuma, N., Nakano, K., Funato, T., et al., 2015. Group motion control of multi-agent systems with obstacle avoidance: column formation under input constraints. *Artif. Life Robot.* 20 (1), 70–77.

- Oberleithner, K., Paschereit, C.O., Seele, R., et al., 2012. formation of turbulent vortex breakdown: intermittency, criticality, and global instability. *AIAA J.* 50 (7), 1437–1452.
- Pan, W.W., Jiang, D.P., Pang, Y.J., et al., 2017. A multi-AUV formation algorithm combining artificial potential field and virtual structure. *Acta Armamentarii* 38 (2), 326–334.
- Perdereau, V., Passi, C., Drouin, M., 2002. Real-time control of redundant robotic manipulators for mobile obstacle avoidance. *Robot. Autonom. Syst.* 41 (1), 41–59.
- Qiu, H., Duan, H., 2014. Receding horizon control for multiple UAV formation flight based on modified brain storm optimization. *Nonlinear Dynam.* 78 (3), 1973–1988.
- Qu, D.K., Du, Z.J., Xu, D.G., et al., 2008. Research on path planning for a mobile robot. *Robot* 30 (2), 97–96.
- Qu, H., Xing, K., Alexander, T., 2013. An improved genetic algorithm with co-evolutionary strategy for global path planning of multiple mobile robots. *Neurocomputing* 120 (10), 509–517.
- Rimon, E., Koditschek, D.E., 1992a. Exact robot navigation using artificial potential functions. *IEEE Trans. Robot. Autom.* 8 (5), 501–518.
- Rimon, E., Koditschek, D.E., 1992b. Exact robot navigation using artificial potential functions. *IEEE Trans. Robot. Autom.* 8 (5), 501–518.
- Sharma, S.K., Sutton, R., Motwani, A., Annamalai, A., 2014. Non-linear control algorithms for an unmanned surface vehicle[J]. *Proc. Inst. Mech. Eng. M: J. Eng. Marit. Environ.* 228, 146–215.
- Shojaei, K., 2015. Leader-follower formation control of underactuated autonomous marine surface vehicles with limited torque. *Ocean Eng.* 105, 196–205.
- Wang, N., Xu, H., 2020. Dynamics-constrained global-local hybrid path planning of an autonomous surface vehicle. *IEEE Trans. Veh. Technol.* 69 (7), 6928–6942.
- Wang, N., Jin, X., Er, M.J., 2019. A multilayer path planner for a USV under complex marine environments. *Ocean Eng.* 184, 1–10.
- Yang, Y., Wang, S., Wu, Z., et al., 2011. Motion planning for multi-HUG formation in an environment with obstacles. *Ocean Eng.* 38 (17), 2262–2269.
- Zuo, L., Yan, W., Cui, R., et al., 2016. A coverage algorithm for multiple autonomous surface vehicles in flowing environments. *Int. J. Contr. Autom. Syst.* 14 (2), 540–548.